VOL. 10, NO. 4, MARCH 2015 ISSN 1819-6608
ARPN Journal of Engineering and Applied Sciences
©2006-2015 Asian Research Publishing Network (ARPN). All rights reserved.
www.arpnjournals.com

A NOVEL SEMI-AUTOMATED 3-D CAD VISUALIZATION SYSTEM AS AN AID FOR SURGICAL PLANNING OF LUNG CANCER

Manikandan T.[1] and Bharathi N.[2]
[1]Department of Electronics and Communication, Engineering, Rajalakshmi Engineering College, Chennai, India
[2]Department of Electrical and Electronics Engineering, Velammal Engineering College, Chennai, India
E-Mail: mani_stuff@yahoo.co.in

ABSTRACT

Lung cancer is the leading cause of cancerous deaths in the world in men and women. It is the most difficult cancer to cure and the number of deaths that it causes is generally increasing. It is very difficult to detect in its early stage. In advanced stages, treating the disease includes surgery, chemotherapy, radiation therapy or combination. Normally, the radiologists and surgeons detect the locations of the cancerous tumor from the computed tomographic images. However, the computed tomographic images are two dimensional. The mapping of stacks of two dimensional images into original lung cavities in three dimensional involves lot of mental work and long time for the surgeons before they plan for surgery. This work aimed to develop a novel semi-automated three dimensional computer-aided diagnostic system to localize the cancerous lung tumor in isotropic chest computed tomographic images. In addition, it measures the volume and size of the cancerous tumor. Low dose helical computed tomographic scan images retrospectively obtained from 23 subjects who suffered from lung cancer (conformed through biopsy test) have been taken for this study. To validate the system performance, results were compared with the three independent radiologist's results. The obtained results show that a computer-aided diagnostic system performance is satisfactory and may useful for surgical planning of lung cancer.

Keywords*:* computed tomography, lung cancer, MIMICS, lobar fissure, lung lobes, 3-D visualization.

1. INTRODUCTION

Lung cancer is considered to be the main cause of cancer deaths in worldwide. It affects 100,000 Americans of the smoking population every year of all age groups, particularly those above 50 years of the smoking population [1-3]. In India, 51,000 lung cancer deaths were reported in 2012, which include 41,000 men and 10,000 women [4]. It is the leading cause of cancer deaths in men; however, in women, it ranked ninth among all cancerous deaths [5]. Lung cancer can be effectively treated if it is diagnosed in its early stages [6-7]. In advanced stages, treating lung cancer is the surgical removal (lobectomy) of the diseased lung lobes [8]. Prior to the actual surgical procedure, accurate planning using anatomic information is very essential.

The essential organ of respiration in humans is the lungs. The anatomy of the human lungs is shown in "Figure-1"; it has five distinct partitions called lobes. The lobes are separated by the lobar fissure. Lobar fissures are the boundaries of the lung lobes where the bronchial trees are absent. The right lung consists of the superior lobe, middle lobe and inferior lobe, which are separated by a right horizontal fissure and right oblique fissure [9]. The left lung consists of superior and inferior lobes which are separated by a left oblique fissure [10]. In general, the functions of the lobes are relatively independent of one another with no major airways or vessels crossing the lobar fissures [11]. Radiographic imaging plays an important role to detect and diagnose the abnormalities in the lungs. Lung nodules are the spots on the lung that are 3cm in diameter or less [12]. In people less than 35 years of age, the probability that a lung nodule is cancerous is less than 1%, whereas above the age of 50 years, half the lung nodules in people are malignant (cancerous). The other factor that lowers or raises lung cancer includes, smoking history, occupation, medical history, shape and growth [13-14]. The primary radiographic imaging tool for lung nodule detection is computed tomography (CT) which has replaced the earlier film-based projection radiography [15]. The cancerous tumor can grow double in size on an average every four months. The growth can be evaluated through a series of CT scans over a period of time [16].

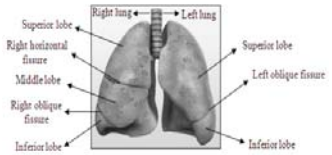

Figure-1. Anatomy of human lung.

For surgical planning, surgeons in current clinical practice, read stacks of clinical CT images (typically about the thickness of 2.5-7.0 mm) for assessing the spatial relationships among anatomic structures of lung cavities, specifically identifying the diseased lung lobes [17]. These CT images offer two dimensional (2D) views from a single view point, and have different shades of gray. Reading CT slices is a highly subjective task and requires enormous mental work to map the anatomic structures from the 2-D images onto the 3-D actual lung cavities. This leads to long planning times, heavy workload and low accuracy in the predicted surgeries [18].

Modern multi-slice high resolution CT (HRCT) scanners produce isotropic CT images, which have pixel dimensions equal to the image thickness of 0.6 mm. These narrow slices could provide anatomical details of the lungs

©2006-2015 Asian Research Publishing Network (ARPN). All rights reserved.

similar to those available from gross pathological specimens [19]. A complete scan of the lung cavity of an average person results in about 300 images. This large number exceeds the surgeon's ability for handling the information. To reduce the work load of the surgeons, several isotropic CT images are combined to get a clinical 2.5-7.0 mm CT image, resulting in the loss of valuable information that could be used for more accurate surgical planning. Further, studies have shown that in such CT images, approximately 70% of the fissures are incomplete, and it is impossible to identify them even by an expert [20-21].

With the appearance of virtual reality techniques, the 3-D visualization of lung cavities is gaining popularity for surgical planning of treating lung diseases [22-23]. In recent years, serious efforts have been made toward the advance of computer aided diagnosis (CAD) systems in diagnostic radiology [24]. In radiology, the CAD system supports the diagnosis made by a clinician (radiologist) who uses the output from a computerized analysis of medical images as a second opinion. Unlike conventional 2-D views, 3-D visualization provides views of the actual lung cavities in three dimensions, where there is no need for mental reconstruction. Recent studies revealed that the 3-D visualization of lung cavities outplayed conventional 2-D CT images for surgical planning. The most important challenge in the 3-D visualization of lung cavities was the extraction of the lobar fissures. This is due to the variable shapes and appearance of fissures along with the low contrast and high noise associated with CT images [25].

To our knowledge, there have been very few studies designed to reconstruct the CT lung images in 3-D environment using CAD systems. Delegacz et. al. have developed a 3-D visualization system to aid physicians observing the abnormalities in human lungs [26]. This algorithm provides better visualization of internal lung structures like bronchi and possible cancer masses. However there were no supporting results for their work. Hu investigated the role of 3-D visualization in the surgical planning of treating lung cancer [18]. By utilizing the software AMIRA (Mercury Computer Systems Inc., France) the author calculated the planning time, workload experienced and accuracy of predicted respectability for surgical planning of treating lung cancer. However, no information was specified about lung cancer localization and its dimensions. Liao et. al described a medical color-enhanced 3-D visualization system for lung cancer detection, based on the volume rendering method [27]. In their work, they identified lung tumor in a 3-D visualization environment, but sacrificed some visual effects to gain the rendering performance. Wei et. al developed a pipelined algorithm based on the modified adaptive fissure sweep and wavelet transform to segment the lung lobes in 2-D environment. In addition, the algorithm describes a procedure for visualizing lung lobes in three dimensions using AMIRA software [28]. Their algorithm allows surgeons to segment the lung lobes in a 3-D environment but there is no evidence about the cancerous tumor location.

The segmentation of lung lobes in isotropic CT images becomes important for utilizing their original details for accurate surgical planning. The isotropic CT images are noisier compared to clinical CT images; however, fissures in the former are accurately visible to the human eyes than in the latter. In this paper we present a lobe segmentation algorithm to segment lung lobes in 0.6 mm isotropic CT images. This paper also describes a procedure for visualizing cancerous tumor in three dimensions, using the software-Meterialise's interactive medical image control system (MIMICS). To describe the 3-D CAD visualization system, we have organized this paper as follows. Section II describes the materials and methods. Section III presents the results and discussion of the lobe segmentation algorithm and 3-D visualization procedure. Finally, section IV gives the conclusion.

2. MATERIALS AND METHODS

The study has been approved by the ethical committee of the Bharat Education and Research Foundation (Academic wing of Bharat Scan), Royapettah, Chennai (Ref:IEC-BERF/Approval Lr./Date: 4-6-2014), and the requirement for informed patient consent was waived in this retrospective study.

Low dose (500 mA & l20 kV), light speed, helical CT scan (General Electric, New York, USA) images retrospectively obtained from 23 (age=62.5±9.8 years) lung cancerous subjects, confirmed through the biopsy test, have been taken for this study. Of these 23 subjects, 14 were males (age=65.14±8.96 years) and 9 were females (age=57.88±10.03 years). The subjects included in the study were those who had cancerous tumor size greater than with a range of 3 cm to 10 cm, determined by one chest radiologist who did not participate in the observer study. A pathology assessment revealed that of the 23 cancerous tumors, 21 were primary lung cancers and 2 were metastatic lung cancers. The CT images obtained retrospectively from 64 slices CT scanner, in which the thickness of each slice was 0.6 mm.

The 3-D visualization system was carried using MIMICS (Developer Version 16.0, Materialize, Belgium) software and its segmentation algorithm [29]. It is an image processing software for 3-D design and modeling developed by materializes. It calculates surface 3-D models from stacked image data such as CT, magnetic resonance imaging (MRI) and ultrasound through image segmentation. The region of interest (ROI) of the image is selected in the segmentation process is converted in to a 3-D surface model using an adapted marching cubes algorithm that take the partial volume effect into account, leading to very accurate 3-D models [30].

A MIMIC accepts stacks of 2-D CT slices and reconstructs them into a 3-D lung model, from which the original lung cavities of human beings can be seen. The flow diagram of such a 3-D CAD visualization system is shown in "Figure-2". This uses two stage approaches for cancerous tumor localization. In first stage, stacks of 2-D CT slices were combined to make 3-D model of the lungs. In second stage, cancerous tumor was segmented from the

©2006-2015 Asian Research Publishing Network (ARPN). All rights reserved.

lung lobes. First, stack of 2-D CT slices were fed to the MIMICS to reconstruct a 3-D lung model. The reconstructed 3-D model of lung consists of soft tissues (lung region) which are surrounded by rib cage. The ROI of this work was focused on cancerous tumor segmentation; hence the lung region was segmented from rib cage for further analysis. Then the lungs were segmented into lung lobes. Then the cancerous tumor was segmented from the lungs and superimposed on the lungs to show its exact location. Various measurements like volume and size of the cancerous tumor was made. Finally, cancerous tumor was superimposed on the lung lobes to show its exact location in 3-D.

The series of steps involved in lung lobe segmentation and 3-D visualization of cancerous tumor were listed below.

A. Histogram Analysis

In two dimensional image processing context, the histogram is normally refers to the frequency of occurrence of gray level values in an image. However in three dimensional image processing context, it gives the frequency of occurrence of voxel (volumetric pixel) vales in a stack of 2-D CT slices. The Hounsfield Unit (HU- a measure of tissue density based on X-ray attenuation in Computed Tomography scanners) is used to measure the voxel values. The lungs consist of soft tissues which are surrounded by rib cage. The HU of soft tissues were different that of HU of rib cages for the lung images. Therefore further processing of lung images were possible based on the histogram analysis.

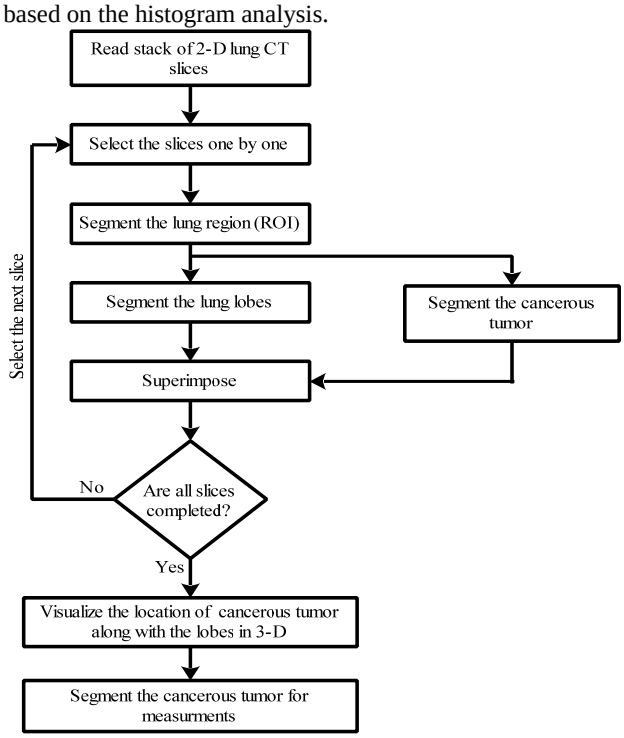

Figure-2. Flow diagram of the 3D CAD visualization system.

B. Thresholding

The next step after the histogram of an image was thresholding. Thresholding plays vital role in image analysis based on HU. Although the HU of bones (rib cage) and air (lungs) vary by huge amounts, they remain fairly constant among patients. Thus, the technique automatically selects a threshold value based on the mean pixel intensity value present in stack of 2-D CT slices. The technique then defines region of interest containing the lungs within the rib cage. This avoids the computation of processing anatomic structures outside the lungs. The voxel values of lungs and rib cage distributed from -825 to 2500 HU. On the images, the areas of rib cage was bright (high voxel value) and the areas of soft tissues were dark (low voxel value). Therefore it was possible to select ROI in a lung images by proper choice of voxel value (threshold).

C. Region growing and calculation of 3D view

The purpose of region growing allows to grow the similar region (similar voxels) to make the 3D model of a lung image. Thresholding technique can be combined with 3-D region growing technique to produce its virtual 3-D lung model. The volumetric pixels corresponding to the soft tissues will have similar values in nature. Similarly, volumetric pixel values corresponding to the rib cage will also have similar values. Grow the regions of soft tissues selected by the proper choice of voxel value (threshold) to make the 3-D model of the same. Similar procedure was used to create 3D model of the rib cage.

D. Segmentation of lung lobes and calculation of 3D view

In most of Computed Tomography images, fissure regions generally appeared as the regions with an absence of vascular and bronchial trees extending from outside boundary to the inside boundary of the lungs. Given a stack of CT slices, we first extracted rib cage and lung regions. For this extraction, we combined thresholding with region growing. Since our aim was segmentation of cancerous tumor, the lung region segmented from rib cage for further processing. The segmentation of lung lobes on lung image was carried out by extracting the lobar fissures. The lobar fissures are the boundaries of lung lobes, which separate all the five lobes in the human lung. Hence the lobar fissures in stack of 2-D lung slices need to be identified for lung lobe segmentation. By segmenting the lung lobes later the location of the cancerous tumor can be identified. The lobe segmentation was carried out separately for all the lobes by multiple slice edit and edit mask techniques on 2-D CT slices. Then 3-D view was calculated for all segmented CT slices. All the segmented lung lobes appear with unique colour in the 3-D model.

E. Cancerous tumor segmentation and tumor measurements

©2006-2015 Asian Research Publishing Network (ARPN). All rights reserved.

The cancerous tumor will grow uncontrolled manner in comparison with benign tumor. The rate of growth can be analyzed through CT scan over the period of times. The cancerous tumor can spread to the other organs and kill them. Finally, it leads to patient's death, if it is not treated. Therefore it is necessary to locate the cancerous tumor for effective treatment, thereby it increases the survival rate of the patients with lung cancer.

The cancerous tumor region was segmented from the lung lobes by dynamic region growing technique. The dynamic region growing technique allows selecting the cancerous tumor in 2-D slices by the proper choice of seed value (similar to voxel of cancerous tumor). The segmented cancerous tumor will have the different colour that of the lung lobes. The 3-D view was calculated for the segmented cancerous tumor along with the lung lobes. The cancerous tumor can be segmented from the lobes for later analysis. Further there is a provision in 3-D model to erase the stray pixels and fill the cavities in the cancerous tumor.

3. RESULTS AND DISCUSSIONS

The input lung CT slices were fed to the input of MIMICS software. The series of steps involved in segmentation of lung lobes for a subject with lung cancer are given in "Figure-3". First, the histogram of the stacks of 2-D slices shows that volumetric pixel values corresponding to the soft tissues (lung region) are different from the rib cage. The voxel values corresponding to the rib cage was selected and combined with region growing technique to make the 3-D model for the rib cage. Similarly, the voxel values corresponding to the lung region was selected and combined with region growing technique to make the 3-D model for the lung along with rib cage which is shown in "Figure-3(a)". Then the soft tissues (ROI) were segmented from the rib cage for further analysis ["Figure-3(b)"]. The lung lobes were segmented from the 3-D lung image by identifying the lobar fissures in the 2-D stacks of CT lung slices, which is shown in "Figure-3(c)". The segmented lung lobes will have unique colour.

The cancerous tumor was segmented from the lung lobes with proper choice of seed value by dynamic region growing ["Figure-4(a)"]. The segmented cancerous tumor will have unique colour, which appears long with the lung lobes. The superior lobe in the left lung was segmented to show the cancerous tumor location. It was evident from "Figure-4(b)" that the cancerous tumor was located in the inferior lobe of a cancerous patient. Further the cancerous tumor was segmented from the lobes for further analysis ["Figure-4(c)"].

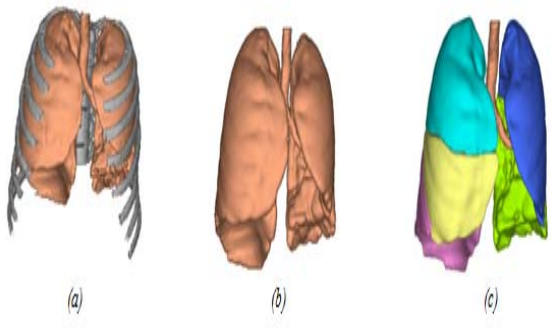

Figure-3. Series of steps involved in lung lobes segmentation.

(a) 3-D model of lung with rib cage
(b) Segmented lung region and
(c) Segmented lung lobes

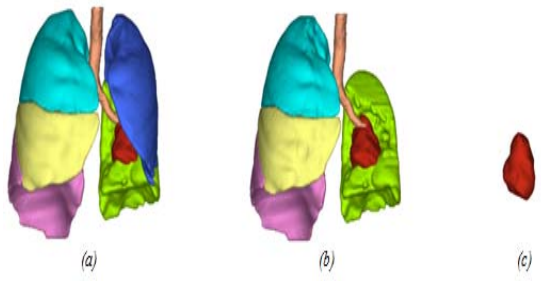

Figure-4. Series of steps involved in segmentation of cancerous tumor.

(a) Lung lobes with cancerous tumor
(b) Segmented lobe shows the tumor location and
(c) Segmented cancerous tumor

The volume and size of the cancerous tumor measured from all the 23 cancerous subjects are given in "table I". Results of cancerous tumor analysis ("Table-I") indicated cancerous tumor size was highest with patient 23 (3.21 cm) and least with patient 12 (9.22 cm), respectively. The calculated mean cancerous tumor size was observed as 4.9 (±1.41) centimeters. There were also noticeable for all other cancerous subjects the tumor size varies between 3.21 and 9.22 centimeters.

©2006-2015 Asian Research Publishing Network (ARPN). All rights reserved.

Table-1. Cancerous Tumor Analysis.

# Patient	Measurements of cancerous tumor	
	Volume (cm^3)	**Size** (cm)
#1	118.28	4.91
#2	56.69	3.84
#3	90.7	4.49
#4	182.48	5.67
#5	124.32	4.99
#6	272.45	6.48
#7	40.93	3.45
#8	193.22	5.78
#9	191.42	5.76
#10	67.04	4.06
#11	100.38	4.65
#12	783.78	9.22
#13	70.69	4.14
#14	41.53	3.46
#15	38.40	3.37
#16	203.74	5.88
#17	220.78	6.04
#18	59.98	3.91
#19	92.52	4.52
#20	45.62	3.57
#21	241.13	6.22
#22	35.23	3.28
#23	33.04	3.21

Three independent radiologists (observers) were asked to localize the lung cancerous tumor from the stacks of 2-D CT lung slices of 23 subjects with lung cancer. The identification of fissures in the isotropic CT images was challenging for them, due to the fissure's variable shape and appearance along with low contrast and high noise association on those images. Therefore, the independent observers failed to locate the fissures on all the cancerous subjects correctly. The first independent observer correctly predicted the cancerous tumor location for 19 cancerous subjects out of all the 23 cancerous subjects. The second and third independent observers correctly predicted 18 and 20 cancerous subjects respectively. This leads to their cancer localization rates of 83%, 78% and 87% respectively. The corresponding localization failure rates were 17% (4/23), 22% (5/23) and 13% (3/23). Success rates and failure rates of localizing the cancerous tumor for the three independent observers are given in "Table II". It was clear from table II highest and lowest success rate obtained by the third and second observers, respectively. However, the success rate of the CAD system was found to be significantly high when compared to all the independent observers. The kappa analysis (SPSS version 17.0) showed fair to good agreement between three independent observers without CAD ("Table III").

The morphological variations of lobar fissures play a vital role in the localization of cancerous tumors in lungs. A few research groups made attempts to study the morphological variations of lung fissures from the cadavers of the south Indian region, and reported that the fissures may be complete or sometimes incomplete [31-33]. This study was focused on the localization of cancerous tumor in subjects with lung cancer. The 3-D visualization system correctly localizes 21 cancerous subjects from the total of 23 cancerous subjects; hence, its localization rate was 91% and its corresponding failure rate was 9%. Of the 23 subjects with lung cancer taken for this study, 14 were males and 9 were females. It was found that the right horizontal fissure was incomplete in 2 of the 14 males. In such a situation, the three independent observers as well as our CAD system failed to locate the cancerous tumor in the right lung.

Table-2. Localization of cancerous tumor.

Localization	Observer 1	Observer 2	Observer 3	CAD
Success rate %	83 (19/23)	78 (18/23)	87 (20/23)	91 (21/23)
Failure rate %	17 (4/23)	22 (5/23)	13 (3/23)	9 (2/23)

Table-3. Kappa values between the observers without CAD.

Kappa	Observer 1	Observer 2	Observer 3
Observer 1	1	0.592**	.503*
Observer 2	0.592**	1	0.735**
Observer 3	0.503*	0.735**	1

Values represented are Pearson's correlation coefficient
$^{**}p < 0.01$.
$^{*}p < 0.05$.

4. CONCLUSIONS

Three dimension based detection and diagnosis plays an important role in significantly improving the surgical planning of treating lung cancer. The advantages of 3-D display over 2-D views help in the surgical planning of treating lung cancer. The surgical removal of the diseased lung lobe is the advanced stage of treating lung cancer. For surgical removal, the surgeon must have an idea of the cancerous tumor location before the actual surgical procedure. The localization rates were calculated and compared with the three independent observers to validate the system performance. The localization rates for observers without CAD systems were 83% (19/23),

©2006-2015 Asian Research Publishing Network (ARPN). All rights reserved.

78% (18/23) and 87% (20/23), respectively. With CAD the localization rate was 91% (19/23). Thus, the 3-D visualization CAD system can be successfully used as an aid, to view and analyze a lung cancer patient's CT slices for surgical planning. In addition it measures the volume and size of the cancerous tumor, which are also important to the surgeons, prior to planning for the surgery.

In future, the lung lobes and cancerous tumor can be automatically segmented from the stack of 2-D lung slices using image processing techniques (MATLAB) and combined with MIMICS to identify the cancerous tumor location in the 3-D lung model.

ACKNOWLEDGEMENTS

We thank Dr. Emmanuvel, Founder chairman & managing director, Dr. Beula Emmanuvel, Member secretary, Institutional Ethics Committee, Dr. J. Mohanasundaram, Executive director, Dr. Prabhakaran, Radiologist, Dr. Vadivelu, Radiologists from Bharat Scans, Chennai, Dr. K. Velavan, Consultant Radiation Oncologist & Chemotherapist/Managing director, Erode Cancer Centre, Dr. Ravisankar, Associate Professor of statistics, Ramachandra Medical College and Research Institute, Ramachandra University, Chennai, Dr. K. Aravind, Radiologist, Mr. Sathish kumar and Mr. Paul, Technicians from PROSCANS, Chennai. We also thank Mr. Santhosh Kumar and Ms. Anu Augusty from MTAB, Chennai.

REFERENCES

[1] Cancer Facts and Figures 2009 by American Cancer Society, Available from: http://www.cancer.org, Assessed on 2009.

[2] Data and Statistics, Available at: http://www.lungusa.org/site/c.dvLUK9O0E/b.33347/, Assessed on 2009.

[3] SEER Stat Fact Sheets, Available at: http://seer.cancer.gov/statfacts/html/lungb.html, Assessed on 2014.

[4] D. Behera. Lung cancer in India, Medicine update 2012. Vol. 22, pp. 401-407, 2012.

[5] Statistics on Lung Cancer, available at http://www.beverlyfund.org/statistics.html, Assessed on 2012.

[6] G.C. Kabat. Recent developments in the epidemiology of lung cancer. Semin Surg Oncol. vol.9, pp. 73–79, 1993.

[7] J.R. Molina., P. Yang., S.D. Cassivi., S.E Schild. and A.A. Adjei. Non-small cell lung cancer: epidemiology, risk factors, treatment, and survivorship. Mayo Clin Proc, vol. 83, pp. 584-594, 2008.

[8] P.E. Schil., B. Balduyck., M.D. Waele., J.M. Hendriks., M. Hertoghs. and et al. Surgical treatment of early-stage non-small-cell lung cancer. European journal of cancer supplements. Vol. 11 (2), pp. 110-122, 2013.

[9] U.G. Esomomu., M.G. Taura., M.H. Modibbo. and A.O. Egwu. Variation in the lobar pattern of the right and left lungs: A case report. The Australian medical journal. Vol. 6 (10), pp. 511-514, 2013.

[10] Lung lobes and lung fissures, Available from: http://www.getbodysmart.com/ap/respiratorysystem/lungs/lobes_fissures/tutorial.html, Assessed on 2011.

[11] Q. Wei., Y. Hu., G. Gelfand. and J.H. MacGregor. Segmentation of Lung Lobes in High-Resolution Isotropic CT Images in IEEE Transactions on Biomedical Engineering. vol. 56, no.5, pp. 1383-1393, 2009.

[12] J.H. Austin., N.L. Mueller., P.J. Friedman., D.M. Hansell., D.P. Naidich. and et al. Glossary of terms for CT of the lungs: recommendation of the Nomenclature Committee of the Fleischner Society. Radiology, vol.200, pp. 327-331, 1996.

[13] Fact sheet on lung cancer, Available from: http://www.cansa.org.za/files/2014/03/Fact-Sheet-Lung-Cancer-March-2014.pdf, Assessed on 2014.

[14] I.J. Lee., G. Gamsu., J. Czum., N. Wu., R. Johnson and et al. Lung nodule detection on chest CT: Evaluation of a computer-Aided detectin (CAD) system Korean journal of radiology. Vol. 6(2), pp. 89-93, 2005.

[15] X.H. Wang., J. E. Durick., A. Lu., D.L. Herbert., C.R. Fuhrman. and et al. Compare display schemes for lung nodule CT screening. Journal of digital imaging, Vol. 24(3), pp. 478-484, 2011.

[16] Pulmonary nodules, Available from: http://www.urmc.rochester.edu/encyclopedia/content.aspx?contenttypeid=22&contentid=pulmonarynodules, Assessed on 2010.

©2006-2015 Asian Research Publishing Network (ARPN). All rights reserved.

[17] E. M. V. Rixoort. and B.V. Ginneken. Automated segmentation of pulmonary structures in thoracic computed tomography scans: a review," Physics in medicine and biology, Vol. 58, pp. 187-220, 2013.

[18] Y. Hu. The role of three dimensional visualization in surgical planning of treating lung cancer. 27th annual IEEE conference on engineering in medicine and biology society. pp. 646-649, 2006.

[19] M.A. Meziane., R.H. Hruban., E.A. Zerhouni., N.F. Khouri., E.K. Fishman. and et al. High resolution CT of the lung parenchyma with pathologic correlation. Radiographics. Vol. 8 (1), pp. 27–54, 2008.

[20] B. N. Raasch., E.W. Carsky., E.J. Lane., J.P. O'Callaghan. and E. R. Heitzman. Radiographic anatomy of the interlobar fissures: A study of 100 specimens. Amer. J. Roentgenol. Vol. 138, pp. 647–554, 1982.

[21] K. Hayashi., A. Aziz., K. Ashizawa., H. Hayashi., K. Nagaoki. and et al. Radiographic and CT appearances of the major fissures. Radiographics. vol. 21, pp. 861–874, 2001.

[22] B.M. Hemminger., P.L. Molina., T.M. Egan., F.C. Detterbeck., K.E. Muller. and et al. Assessment of real-time 3D visualization for cardiothoracic diagnostic evaluation and surgery planning. J. Digit. Imag. Vol. 18, pp. 145-153, 2005.

[23] Y. Hu. and R. A. Malthaner. The feasibility of three-dimensional displays of the thorax for preoperative planning in the surgical treatment of lung cancer. Eur. Cardio-Thorac. Surg. Vol. 31, pp. 506-511, 2007.

[24] W.R Webb., N.L. Muller. and D. P. Naidich. High-Resolution CT of the lung. 3rd ed. Plilandelphia, PA: Lipponcott, Williams and Wilkins, 2001.

[25] Q. Wei., Y. Hu., J. H. Macgregor. and G. Gelfand. Segmentation of lung lobes in clinical CT images. International Journal of Computer Assisted Radiology & Surgery. Vol. 3, pp. 151-163, 2008.

[26] A. Delegacz., S.C.B. Lo., H. Xie. and M.T. Freedman. Three-dimensional visualization system as an aid for lung cancer detection. Proc. Of SPIE, Image Display and Visualization. vol. 3976, pp. 401-409, 2000.

[27] H.S. Liao., P.Y. Li., C.W Ku., K. Tsai. and C.Y. Sun. Diagnoses and surgical planning of lung cancer in color-enhanced 3D visualization system. Proceeding of international conference on Asia Pacific association for medical informatics. pp. 60-67, 2006.

[28] Q. Wei., Y. Hu., G. Gelfand. and J.H. MacGregor. Segmentation of lung lobes in High-Resolution Isotropic CT Images. IEEE Trans. Bimed Engg. vol.56 (5), pp.1383-1392, 2009.

[29] Mimics innovation suite community, Available from: http://uc.materialise.com/MIMICSs/, Assessed on 2012.

[30] N.E. Wiener. Extrapolation, Interpolation, and Smoothing of Stationary Time Series, with Engineering Applications. Cambridge, MA: MIT Press, 1949.

[31] A.P. Geasase. The morphological fissures of major and accessory fissures observed in different lung specimens. Morphologie, vol. 90, no.288, pp. 26-32, 2006.

[32] Prakash., B. Ajay Kumar., M. Sasirekha., H.Y Suma., K. Gowtham. and Gajendra Singh. Lung Morphology: a cadaver study in Indian population. IJAE, vol. 115(3), pp. 235-240, 2010.

[33] J. Suja Mary. and M. Pillay. Variations in the inter-lobar fissures of lungs obtained from cadavers of south Indian origin. International journal of morphology. Vol. 31(2), pp. 497-499, 2013.